Available online at www.sciencedirect.com

ScienceDirect

Journal of Electrical Systems and Information Technology 3 (2016) 45–67

www.elsevier.com/locate/jesit

Analyzing the effect of dynamic loads on economic dispatch in the presence of interline power flow controller using modified BAT algorithm

Y.N. Vijay Kumar [a,*], Sirigiri Sivanagaraju [b], Chintalapudi V. Suresh [b]

[a] *Department of Electrical and Electronics Engineering, SVCET, Chittoor, A.P., India*

[b] *Department of Electrical and Electronics Engineering, Vasireddy Venkatadri Institute of Technology, Nambur, Guntur, A.P., India*

Received 21 January 2015; received in revised form 14 March 2015; accepted 26 August 2015

Available online 24 March 2016

Abstract

Now a day, non-uniform increase of demand on a power system turns the research toward the dynamic analysis. In this paper, to perform dynamic analysis and to solve economic load dispatch problem using optimal power flow (OPF), four realistic load levels are considered. Further, the effectiveness of the objective has been enhanced in the presence of interline power flow controller (IPFC). An optimal location identification methodology for IPFC based on line stability index (LSI) is also presented. The effect of ramp-rate limits on generations and the effect of dynamic loads on generation fuel cost and transmission losses are also analyzed on standard IEEE-30 bus and real time 23 bus test systems with supporting validations, numerical and graphical results.

Keywords: Interline power flow controller; Power injection modeling; Modified BAT algorithm; Dynamic loads; Economic dispatch problem

1. Introduction

The present power system is operating closed to their thermal and stability limits to optimize the economy, environmental, power losses, voltage stability and reliability considerations. The present utility on the system increases the utilization of the existing transmission network and sometimes leads to insecure operation. It is very clear that, if the transfer capability of transmission network is increased, and security is decreased and gradually system becomes more complex. There are various criterions to meet the increasing load by satisfying stability and reliability aspects. In conventional power system, because of the sudden changes in load could leads to instability and this problem can be minimized in the presence of FACTS controllers. Finally, the system in the presence of FACTS can increase the

* Corresponding author.

E-mail addresses: yn.vijaykumar@gmail.com (Y.N. Vijay Kumar), venkatasuresh3@gmail.com (C.V. Suresh).

Peer review under responsibility of Electronics Research Institute (ERI).

Production and hosting by Elsevier

http://dx.doi.org/10.1016/j.jesit.2015.08.003

power system capability to handle rapid changes in operating conditions of the system as well. Using these devices, it is possible to obtain controlled power flow and improved transmission security.

The basic concept of these controllers was developed by Hingorani in 1988 (Hingorani, 1988). There are different types of FACTS controllers based on the type of connection, such as series, shunt, series-series, series-shunt type of connections. The effective modeling of these devices to place them in a given network is presented with supporting mathematical derivations. In general these controllers are mathematically developed using two approaches. One out of this is based on variable reactance model and the other one is variable firing angle model (Acha et al., 2004). Using these devices, it is possible to control the voltage angle and magnitude at the system buses and the power flow through the transmission lines by varying the transmission line impedance of transmission system (Hingorani and Gyugyi, 1999).

The following literature is concentrated in modeling various FACTS controllers (Gotham and Heydt, 1998; Kumari et al., 2007). The performance of the power system under steady-state and dynamic states to enhance the voltage profile and in terms of voltage/angle stability was presented in Kirschner et al. (2005), Yan and Singh (2001), Perez et al. (2000), Xingbin et al. (2003) and Pilotto et al. (1997). Modeling of voltage source converter (VSC) based FACTS controller like UPFC and IPFC for power flow analysis is presented in Xia Jiang et al. (2008). The efficient and load flow algorithms were developed in Padhy and Abdel Moamen (2005), Douglas et al. (1998), Yan and Sekar (2005), Fuerte-Esquivel and Acha (1996) and Xiao et al. (2002) to place these devices in a given network. From the literature, it is identified that, multi-line FACTS controllers are more effective than that of single line FACTS controllers. In this regard, a model of interline power flow controller (IPFC) for OPF to solve line over load problem to minimize generation fuel cost is proposed in Teerathana et al. (2005). IPFC power injection model for congestion management and total active power loss minimization in electric power system is presented in (Jun and Yokoyama, 2006a). An indirect unified power flow controller model to enhance reusability of Newton power flow codes is proposed in Bhowmick et al. (2008). A current based model of static synchronous series compensator and IPFC was presented in Vinkovic and Mihalic (2008, 2009). A power injection model of IPFC for load flow analysis with practical constraints such as maximum series injected current or voltage and maximum active power exchange on the DC link is presented in Yankui et al. (2006). The power injection model of FACTS deices like UPFC and IPFC has been focused in Jun and Yokoyama (2006b). Sensitivity methods (Xinghao et al., 2009), various heuristic evolutionary optimization algorithms (Deng and Lie, 1995) were proposed to identify an optimal location and parameter settings of IPFC.

Recent years, many blackouts are due to the uneven increment of load on a system without considering the stability of the system. The system performance needs to be studied with some the factors such as voltage regulation, rotor angle stability, reactive power compensation, protective relaying, reactive power management, etc. Finally, from this, the load on a system should be increased by maintaining certain amount of the reserve capacity to avoid mal operations during small disturbances. The shunt type FACTS controllers are placed based on the reactive power flow margin and voltage stability proximity index is proposed in Sauer et al. (1993) and Lof et al. (1993).

From the past few decades, most of the research was concentrated to solve optimal power flow problem in the presence of various FACTS controllers. In general, the OPF problem with series compensation increases the complexity of the problem and the conventional optimization techniques cannot converge to local minima (Taranto et al., 1992). To overcome this problem, genetic algorithm and hybrid tabu search and simulated annealing optimization algorithms are proposed in Chung and Li (2001) and Ongsakul and Bhasaputra (2002). The optimal power flow with FACTS controllers increases the complexity of the problem. The optimal location of these controllers and the economic load dispatch problems are solved using enhanced bacterial foraging algorithm (EBFA) in Belwin Edward et al. (2013). The optimal location and the parameters of the FACTS controllers are identified by minimizing the generation fuel cost along with the device installation cost is proposed in Singh and David (2001).

There are conventional methods based on linear and non-linear programming, Lagrange relaxation, dynamic programming and quadratic programming (Hindi and Ab Ghani, 1991) are proposed to solve dynamic economic dispatch (DED) problem. These methods are suffering from premature convergence at local optimal solution. Recently, stochastic optimization algorithms such as evolutionary programming (EP) (Shanti Swarup and Natrajan, 1994), simulated annealing (Panigraphi et al., 2006), differential evolution (DE) (Hao et al., 2007), modified EP-SQP (Titus and Ebenezer Jeyakumar, 2008), improved PSO (Baskar and Mohan, 2008), and hybrid swarm intelligence based algorithms (Attaviriyanupap et al., 2002) have been used to solve DED problem with convex fuel cost as an objective.

From the careful review of the literature, it is identified that, the realistic loads on economic load dispatch should be analyzed to identify the effect of the same. For this, the minimum, base, average and peak loads are considered to

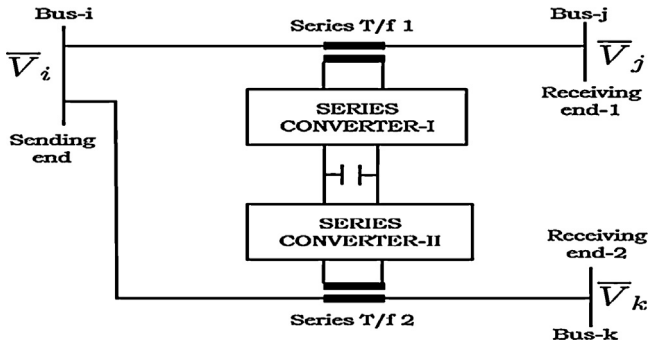

Fig. 1. Schematic representation of IPFC.

be the more realistic loads on a given system. IPFC is capable of controlling power flow in multiple transmission lines simultaneously. Solving the OPF problem in the presence of IPFC increases the complexity of the problem; hence a modified BAT algorithm is presented in this paper. And also, the effect of IPFC should be analyzed on these dynamic loads using OPF problem. In this paper, an optimal location identification methodology to install IPFC based on line stability index (LSI) is also presented. The effectiveness of the proposed methodology is tested on standard IEEE-30 bus and real time 23 bus test systems with supporting numerical and as well as graphical results.

2. Interline power flow controller

In this section, the steady-state modeling of interline line power flow controller (IPFC) is presented with supporting mathematical derivations. This modeling uses the voltage source based power injections commonly known as power injection modeling. This modeling is used to incorporate IPFC in conventional Newton Raphson load flow solution to identify the effect of the same. The steady state representations of two voltage sources are connected in series with coupling transformer impedance.

2.1. Operating principle of IPFC

The general steady-state model of IPFC consist two back to back connected voltage source converters. These converters are connected in series with the transmission lines via two coupling transformers. The series compensation for two different transmission lines is provided through these transformers. Simply, the IPFC can be represented as coordinated operation of two static synchronous series compensators connected in two different transmission lines. In IPFC, the two voltage source converters are connected via a common DC link. This helps to balance the power exchange between these two converters. The basic schematic representation of IPFC is shown in Fig. 1. It is assumed that, IPFC is connected in two different transmission lines between buses i, j and k with bus-i is common for both lines.

2.2. Power injection model of IPFC

The complete power injection model of IPFC is derived using the voltage source based power injection model. The basic two voltage source converters are compensating two different transmission lines through series coupling transformers having voltage magnitude and respective voltage angles. The equivalent voltage source based representation of IPFC is shown in Fig. 2. In this modeling, it is assumed that, the voltage source converters are injecting almost sinusoidal voltage with controllable voltage magnitude and angle.

From Fig. 2, the complex bus voltage magnitudes at IPFC connected buses can be represented as

$$\overline{V_m} = \overline{V_m} = |V_M| \angle \delta_m; \quad \forall \quad m = i, j, k \tag{1}$$

Similarly, the complex voltage magnitudes injected by the series converters can be represented as

$$\overline{V}_{se,in} = r_{in} \overline{V}_i e^{j\gamma in}; \quad \forall \quad n = j, k \tag{2}$$

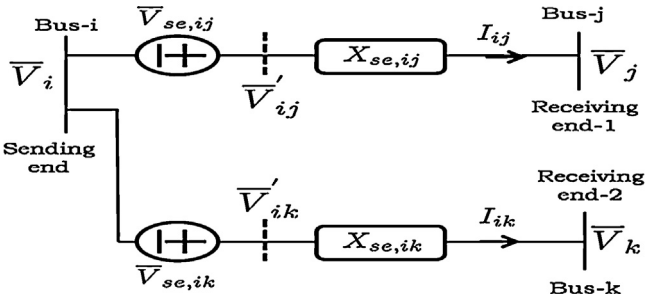

Fig. 2. Equivalent voltage source model of IPFC.

Here, r_{in} and γ_{in} are the respective per unit voltage magnitudes and angles of the respective series connected transformers and these are operating within the following range

$$0 \le r_{in} \le r_{in}^{\max}; \quad \forall \quad n = j,k \quad \text{and} \quad 0 \le \gamma_{in} \le \gamma_{in}^{\max}; \quad \forall \quad n = j,k$$

In this problem, $r_{in}^{\max}$ and $\gamma_{in}^{\max}$ are taken as 0.1° and 360°. The voltage at the fictitious bus i.e. voltage behind the reactance of the coupling transformer can be represented as

$$\overline{V'_{in}} = \overline{V_i} + \overline{V_{se,in}}; \quad \forall \quad n = j,k \tag{3}$$

For the sack of simplicity, it is assumed that, the resistance of the series coupling transformers is neglected. Hence, $X_{se,ij}$, $X_{se,ik}$ are the coupling transformers reactance's respectively. The admittance of the respective coupling transformers can be calculated as

$$B_{se,in} = \frac{1}{X_{se,in}}; \quad \forall \quad n = j,k \tag{4}$$

The final steady state power injection model is developed by converting equivalent voltage source model into equivalent current source model shown in Fig. 3 using Norton's transformation. Then the equivalent current sources of the respective series voltage sources can be expressed as

$$\overline{I}_{se,in} = -jB_{se,in}\overline{V}_{se,in}; \quad \forall \quad n = j,k \tag{5}$$

Using Eq. (2), the equivalent Norton's current can be calculated as

$$\overline{I}_{se,in} = -jr_{in}B_{se,in}\overline{V}_i e^{j\gamma_{in}}; \quad \forall \quad n = j,k \tag{6}$$

Using this, the complex power injected at IPFC sending end bus can be represented as

$$\begin{aligned}\bar{S}_i^{IPFC} &= \overline{V}_i\left(-\overline{I}_{se,ij} - \overline{I}_{se,ik}\right)^* = -\overline{V}_i\left[-jr_{ij}B_{se,ij}\overline{V}_i e^{j\gamma_{ij}} - jr_{ik}B_{se,ik}\overline{V}_i e^{j\gamma_{ik}}\right]^* \\ &= V_i^2\left(r_{ij}B_{se,ij}e^{-j(90^\circ+\gamma_{ij})} + r_{ik}B_{se,ik}e^{-j(90^\circ+\gamma_{ik})}\right)\end{aligned}$$

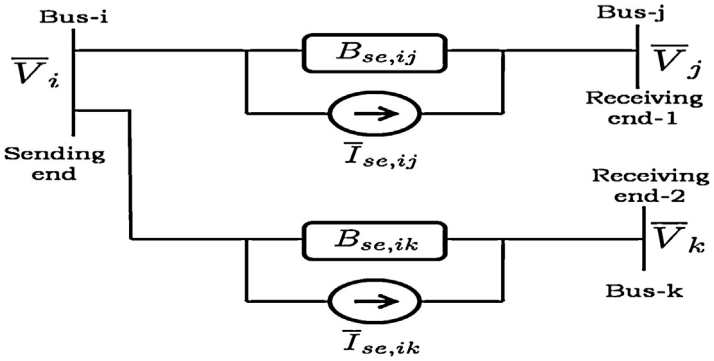

Fig. 3. Equivalent current source model of IPFC.

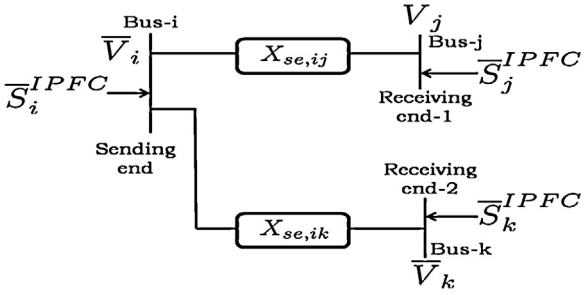

Fig. 4. Equivalent power injection model of IPFC.

Similarly, the power injected at IPFC receiving end buse can be represented as

$$\bar{S}_n^{IPFC} = \overline{V}_n\left(\overline{I}_{se,in}\right)^*; \quad \forall \quad n = j,k = \overline{V}_n\left[-jr_{in}B_{se,in}\overline{V}_i e^{j\gamma_{in}}\right]^* = -V_i V_n r_{in} B_{se,in} e^{-j(90^\circ+\delta_i-\delta_n+\gamma_{in})}$$

Using these equations, the final steady state power injection model of IPFC is shown in Fig. 4 and the real and reactive power injections at respective IPFC buses can be expressed as

$$P_i^{IPFC} = -V_i^2(r_{ij}B_{se,ij}\ \sin\ \gamma_{ij} + r_{ik}B_{se,ik}\ \sin\ \gamma_{ik}) \tag{7}$$

$$Q_i^{IPFC} = -V_i^2(r_{ij}B_{se,ij}\ \cos\ \gamma_{ij} + r_{ik}B_{se,ik}\ \cos\ \gamma_{ik}) \tag{8}$$

$$P_n^{IPFC} = V_i V_n r_{in} B_{se,in}\ \sin(\delta_{in} - \gamma_{in}) \quad \forall \quad n = j,k \tag{9}$$

$$Q_n^{IPFC} = V_i V_n r_{in} B_{se,in}\ \cos(\delta_{in} - \gamma_{in}) \quad \forall \quad n = j,k \tag{10}$$

where, $\delta_{in} = \delta_i - \delta_n$. Finally, it is necessary to satisfy the power balance equation of IPFC, for that, the apparent power supplied by the two series converters can be calculated as

$$S_{ser,in} = V_{se,in}I'_{in} = r_{in}V_i e^{j\gamma_{in}}\left|\frac{V'_{ij} - V_n}{jX_{se,in}}\right|^*; \quad \forall \quad n = j,k$$

Using Eq. (3), the active and reactive power flows supplied by the series converters can be expressed as

$$P_{ser,in} = r_{in}B_{se,in}V_i V_n\ \sin(\delta_{in} + \gamma_{in}) - r_{in}B_{se,in}V_i^2\ \sin(\gamma_{in}); \quad \forall \quad n = j,k$$

$$Q_{ser,in} = -r_{in}B_{se,in}V_i V_n\ \cos(\delta_{in} + \gamma_{in}) + r_{in}B_{se,in}V_i^2\ \cos(\gamma_{in}) + r_{in}V_i^2 B_{se,in}; \quad \forall \quad n = j,k$$

Finally, the IPFC neither generates nor absorbs active power with respect to the system, hence the necessary condition that, the IPFC should satisfy is

$$P_{ser,ij} = -P_{ser,ik}$$

2.3. Incorporation of IPFC model in Newton Raphson algorithm

To incorporate IPFC in a given network, the conventional system equation in Newton Raphson load solution should modify to show the impact of the device. The developed power injection model is easy to incorporate in a given power system by modifying the Jacobian and power mismatch equations at the IPFC connected buses. The final steady state network equation in the presence of this device can be expressed as

$$\left(\begin{bmatrix}\Delta P\\ \Delta Q\end{bmatrix} + \begin{bmatrix}P^{IPFC}\\ Q^{IPFC}\end{bmatrix}\right) = \left(\begin{bmatrix}H & N\\ J & L\end{bmatrix} + \begin{bmatrix}H^{IPFC} & N^{IPFC}\\ J^{IPFC} & L^{IPFC}\end{bmatrix}\right) \quad \begin{bmatrix}\Delta\delta\\ \frac{\Delta V}{V}\end{bmatrix} \tag{11}$$

where, ΔP, ΔQ are the respective power mismatch vectors, $\Delta\delta$, ΔV are the vector increments with respect to voltage magnitude and angles, H, N, J, and L are the first order partial derivatives with respect to δ and V respectively.

The respective power mismatch equations and Jacobian elements correspond to IPFC connected buses are given in Appendix.

3. OPF problem formulation

The generalized form of optimal power flow (OPF) problem can be formulated by considering total power losses as an objective, by adjusting the system control variables while satisfying a set of operational constraints. Therefore, the OPF problem can be formulated as follows:

$$\begin{aligned} &\text{minimize} \quad A(x,u) \\ &\text{Subjected to} \quad g(x,u)=0; \quad h(x,u)\le 0 \end{aligned} \tag{12}$$

where 'g' and 'h' are the equality and inequality constraints respectively and 'x' is a state vector of dependent variables such as slack bus active power generation ($P_{g,slack}$), load bus voltage magnitudes (V_L) and generator reactive power outputs (Q_G) and apparent power flow in lines (S_l) and 'u' is a control vector of independent variables such as generator active power output (P_G), generator voltages (V_G), transformer tap ratios (T) and reactive power output of VAr sources (Q_{sh}).

The state and control vectors can be mathematically expressed as

$$x^{\mathrm{T}} = \left[P_{G1}, V_{L1}, \ldots\ldots, V_{L_{NL}}, Q_{G1}, \ldots\ldots, Q_{G_{NG}}, S_{l1}, \ldots, S_{l_{nt}}\right]$$

$$u^{\mathrm{T}} = \left[P_{G2}, \ldots, P_{G_{NG}}, V_{G1}, .., V_{G_{NG}}, Q_{sh1}, \ldots, Q_{sh_{NC}}, T_1, \ldots, T_{NT}\right]$$

where, '*NL*', '*NG*', '*nl*', '*NC*' and '*NT*' are the total number of load buses, generator buses, transmission lines, VAr sources and regulating transformers respectively.

In practice, the load on a given system is not constant over a specified period. To analyze the effect of variable load on OPF, in this problem, four different load levels are considered. These load levels may present in real power system in most of the time intervals. Conventionally, these load levels are obtained by increasing the both active and reactive loads at all buses by a constant factor. In general, these load levels represents, minimum, base, average and peak loads throughout a specific time interval.

3.1. Dynamic non-convex fuel cost

The generation fuel cost including valve-loading effects for dynamic loads can be expressed as

$$A_{cost,m} = \sum_{i=1}^{NG} \left(a_i P_{G_{i,m}}^2 + b_i P_{G_{i,m}} + c_i + \left|e_i \sin\left(f_i\left(P_{G_i}^{\min} - P_{G_{i,m}}\right)\right)\right|\right); \quad \$/h \quad \forall m = 1, \ldots\ldots, LF \tag{13}$$

where, a_i, b_i, c_i are the fuel cost coefficients of ith unit and e_i, f_i are the cost coefficients related to ramp-rate limits. $P_{G_i}^{\min}$ and P_{G_i} are the minimum generation level and the current active power output of ith generator, '*LF*' is the total number of load levels.

3.2. Constraints

This problem is optimized while satisfying the following equality, in-equality, and practical constraints.

3.2.1. Equality constraints

These constraints are typically power flow equations handled in Newton Raphson load flow.

$$P_{Gi,m} - P_{Di,m} - \sum_{j=1}^{N_{bus}} \left|V_{i,m}\right| \left|V_{j,m}\right| \left|Y_{ij,m}\right| \cos(\theta_{ij,m} + \delta_{j,m} - \delta_{i,m}) = 0$$

$$Q_{Gi,m} - Q_{Di,m} - \sum_{j=1}^{N_{bus}} \left|V_{i,m}\right| \left|V_{j,m}\right| \left|Y_{ij,m}\right| \sin(\theta_{ij,m} + \delta_{j,m} - \delta_{i,m}) = 0$$

where, $P_{Gi,m}$, $Q_{Gi,m}$ are the active and reactive power generations at ith bus in mth load level, $P_{Di,m}$, $Q_{Di,m}$ are the active and reactive power demands at ith bus in mth load level, N_{bus} is the total number of buses and $\left|Y_{ij,m}\right|$, $\theta_{ij,m}$ are the bus admittance magnitudes and its angles between ith and jth buses in mth load level, $|V_{i,m}|$, $|V_{j,m}|$ and $\delta_{i,m}$, $\delta_{j,m}$ are the voltage magnitudes and respective angles at ith and jth buses in mth load level. Here, $m = 1, 2, \ldots, LF$, 'LF' is the total number of load levels.

3.2.2. In-equality constraints

Generator limits

Generator bus voltage limits: $V_{Gi}^{\min} \le V_{Gi,m} \le V_{Gi}{}^{\max}; \quad \forall i \in NG$

Active power generation limits: $P_{Gi}^{\min} \le P_{Gi,m} \le P_{Gi}^{\max}; \quad \forall i \in NG$

Reactive power generation limits: $Q_{Gi}^{\min} \le Q_{Gi,m} \le Q_{Gi}^{\max}; \quad \forall i \in NG$

Security limits

Transmission line flow limit: $S_{li,m} \le S_{li}^{\max}; \quad i \in nl$

Load bus voltage magnitude limits: $V_i^{\min} \le V_{i,m} \le V_i^{\max}; \quad \forall i \in NL$

Other limits

Transformers tap setting limits: $T_i^{\min} \le T_{i,m} \le T_i^{\max}; \quad \forall i \in NT$

Capacitor reactive power generation limits: $Q_{sh_i}^{\min} \le Q_{sh_i m} \le Q_{sh_i}^{\max}; \quad \forall i \in NC$

Ramp-rate limits

The constraints of the ramp-rate limits, the operating limits of the generators are restricted to operate always between two adjacent periods forcibly. The ramp-rate constraints are

$$\max\left(P_{Gi}^{\min}, P_{Gi}^{0} - DR_i\right) \le P_{Gi,m} \le \min\left(P_{Gi}^{\max}, P_{Gi}^{0} + UR_i\right) \tag{14}$$

where, $P_{G_i}^0$ is ith unit power generation at previous hour, DR_i and UR_i are the respective down and up ramp-rate limits of ith unit in mth load level.

3.2.3. Device limits

The following limits are considered for IPFC control parameters:

$$0 \le r_{ij}, r_{ik} \le r^{\max}(0.1\,p.u.)$$

$$0 \le r_{ij}, r_{ik} \le r^{\max}(360^{\circ})$$

$$0 \le X_{se,ij}, X_{se,ik} \le X_{se}^{\max}(0.1\,p.u.)$$

Here, PG, VG, T, Qsh inequality constraints are self restricted constraints and can be satisfied forcibly within the OPF problem, where as the remaining three constraints and active power generation at slack bus are non-self restricted constraints and these can be handled using penalty approach. With this, the generalized form of the OPF problem defined as

$$A_{aug}(x,u) = A(x,u) + \lambda_p\left(P_{G_{1,m}} - P_{G1}^{\lim\, it}\right)^2 + \lambda_v\sum_{k=1}^{NL}\left(V_{k,m} - V_k^{\lim\, it}\right)^2 + \lambda_q\left(Q_{G_{k,m}} - Q_{Gk}^{\lim\, it}\right)^2 + \lambda_s\sum_{k=1}^{nl}\left(S_{l_{k,m}} - S_{l_k}^{\max}\right)^2 \tag{15}$$

where, λ_p, λ_v, λ_q, and λ are the penalty quotients having large positive value. The limit values are defined as

$$x^{\lim\, it} = \left\{\begin{matrix} x^{\max}; x > x^{\max} \\ x^{\min}; x < x^{\min} \end{matrix}\right\}$$

Here 'x' is the value of P_{G1}, V_m and QG_m.

4. Proposed modified BAT algorithm

Bats are the fascinating animals having wings that can fly and have extended capability of echolocation. The algorithm developed using the behavior of bats is usually termed as BAT algorithm. Simply, this algorithm is a metaheuristic population based optimization algorithm. This algorithm basically inspired from the behavior of bats in searching their food/prey using echolocation process. In this process, bats send some signals to the environment and listens its echo signals. Based on this process, the position of food/prey is identified by the bats. Based on the time between the time of emission and the time of echo determines the nearby objects. To make the problem simplicity, the following assumptions are considered (Xin-She Yang and Xingshi He, 2013)

1. Echolocation is the process that all bats are using to identify the distance from its current position to food position.
2. Each bat has its own parameters such as velocity, position, frequency, wavelength and loudness to search the food.
3. All these bats adjust its wavelength/frequency of their emitted pulses.
4. Loudness varies from maximum value to minimum value.

At first, generate the initial population of problem control variables. For the sack of explanation, the following objective function and the respective control variables are expressed as

$$A_i = f(x_{1i}, x_{2i}, \ldots, x_{mi}) \quad \forall i = 1, 2, \ldots, n$$

where, 'm' is the total number of control variables, A_i is the objective function value of ith population and 'n' is the total number of populations. The simple exemplification is given below

$$\begin{bmatrix} A_1 \\ A_2 \\ \vdots \\ A_n \end{bmatrix} = \begin{bmatrix} f(x_{11}, x_{21}, \ldots, x_{m1}) \\ f(x_{12}, x_{22}, \ldots, x_{m2}) \\ \vdots \\ \vdots \\ f(x_{1n}, x_{2n}, \ldots, x_{mn}) \end{bmatrix}$$

For each of the population, calculate the frequency values which are generated between fr_{min} and fr_{max} fr_{max} using the following expression

$$fr_{mn} = fr_{\min} + (fr_{\max} - fr_{\min})\beta$$

where, β is a random number between '0′ and '1′. The fitness values for the respective population can be calculated using

$$fit_i = \frac{1}{1 + A_i}$$

The respective velocities of each of the control variables is calculated using respective minimum ($x_{mn}^{\min}$) and maximum ($x_{mn}^{\max}$) values. The velocity of each of the control variable before starting iterative process (i.e. at "$t-1''$) can be expressed as

$$Vel_{mn}^{t-1} = \frac{\left(x_{mn}^{\max} - x_{mn}^{\min}\right)}{Range} \tag{16}$$

where, '*Range*' is a constant can be considered as 10. In conventional BAT algorithm, the velocity of each of the bat can be calculated in iterative process using the following expression

$$Vel_{mn}^{t} = Vel_{mn}^{t-1} + \left(x_{mn}^{t-1} - x_{mn}^{Gbest}\right) fr_{mn} \tag{17}$$

Here, x_{mn}^{t-1} and x_{mn}^{Gbest} are the current and global best positions of a variable. In the proposed modified BAT (MBAT) algorithm, the velocity is calculated using the following expression

$$Vel_{mn}^{t} = Vel_{mn}^{t-1} + C_1 \left(x_{mn}^{t-1} - x_{m}^{Gbest}\right) fr_{mn} + C_2 \left(x_{mn}^{Gworst} - x_{mn}^{t-1}\right) fr_{mn} \tag{18}$$

Due to this process, each variable tries to achieve best position and tries to avoid the bad experiences. Here, C_1 and C_2 are the chaotic constants can be calculated using the following expression

$$C_1 = C_2 = 1 + \frac{1}{1 + e^{iter}}$$

where, '*iter*' is the current iteration number. In each of the iterations, the position of each of the control variables is updated using

$$x_{mn}^{t} = x_{mn}^{t-1} + Vel_{mn}^{t} \tag{19}$$

Generate one random number (PR) and if this value is greater than 0.1, then, the loudness and rate of pulse emission of each of the bats is calculated using

$$Loud_i^t = \alpha Loud_i^{t-1} \tag{20}$$

$$r_i^t = r_i^{t-1}[1 - e^{-\gamma(t-1)}] \tag{21}$$

Here, α, γ are the constants considered to be 0.9 and initial loudness starts from maximum value i.e. 1 (one) and reaches to minimum value i.e. 0 (zero) or any value between 0 and 1. In MBAT algorithm the constant 'α' in the iterative process is calculated using the following expression

$$\alpha^t = \alpha^{old}(0.5 \times iter)^{1/iter}$$

Due to this process, the ability of the proposed algorithm is to escape from the local optimal solution and to avoid the premature convergence.

Once again, if the rate of pulse is less than the random number and if the local search part is completed; a new set of population is obtained using the random walk

$$x_{mn}^{t} = x_{mn}^{t-1} + \in Loud_{avg}^{t} \tag{22}$$

Here, ϵ is a random number between -1 and 1, $Loud_{avg}^{t}$ is the mean of the loudness of all bats.

The complete flow chart of the proposed modified bat algorithm is shown in Fig. 5.

5. Optimal location of IPFC

In general, to obtain maximum benefit from IPFC, it is necessary to identify an optimal location to install this device in a given system. Here, IPFC is a multi line FACTS controllers, it requires two different transmission lines with a common bus to install the same. So, the conventional optimal location identification methodologies are not suitable to identify an optimal location. Mostly, this device is used to control the power flow in the transmission lines by varying the compensation using voltage source converter. Because of this, the power flow in some of transmission lines gets increased and in some of the transmission lines gets decreased. In this paper, line stability index based location is identified and the complete details are given below:

5.1. Line stability index (LSI) location

From the literature, the severity index (Xinghao et al., 2009) is calculated based on the active/apparent power flows in transmission lines. Even though, severity index and ranking methods are popular and have certain disadvantages. It cannot consider the stability of a transmission line into consideration. Hence in this paper, a new procedure is developed to identify an optimal location based line stability index (LSI). This index directly represents the stability of the system

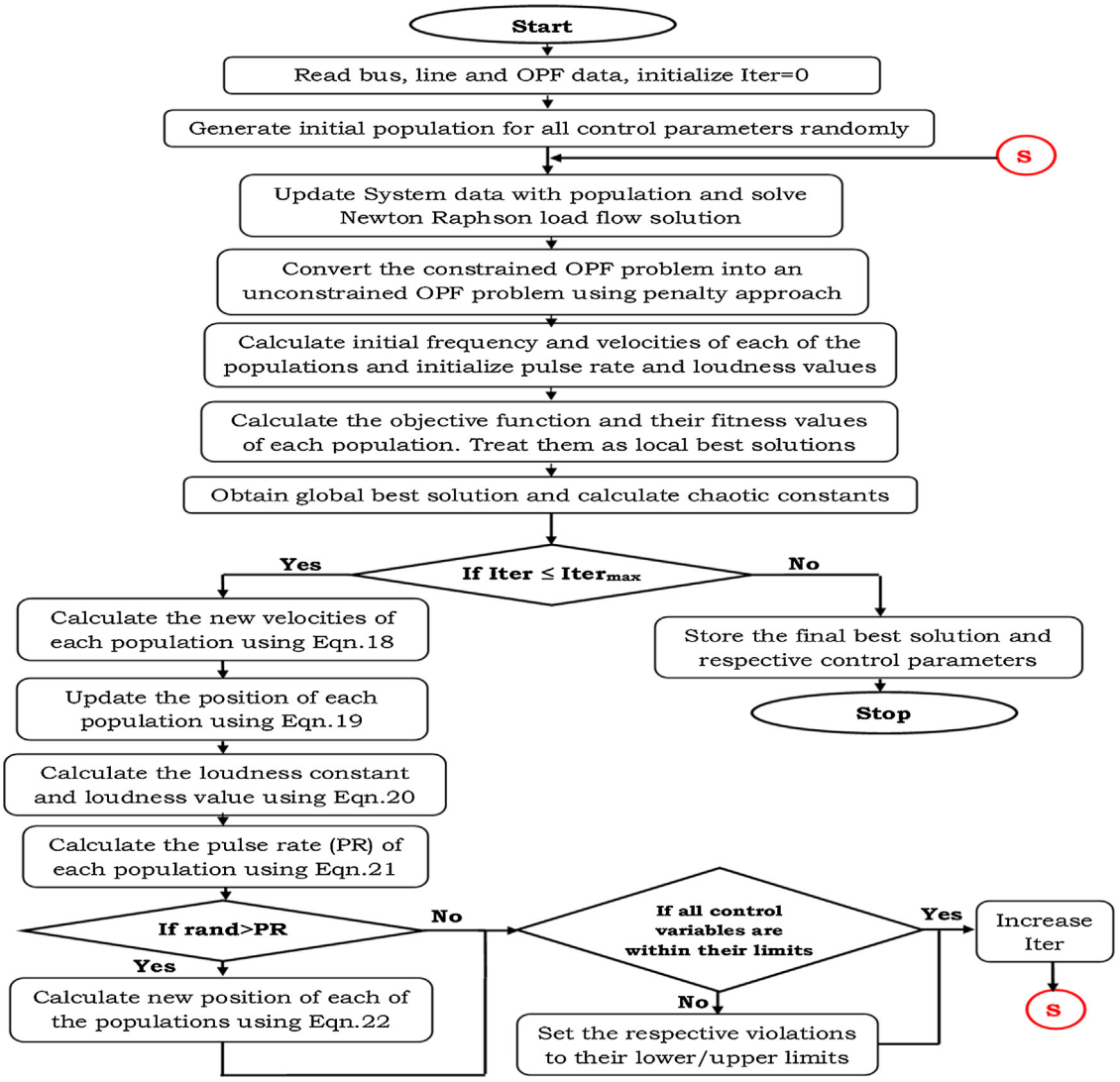

Fig. 5. Flow chart of the proposed MBAT algorithm.

in terms of line loadings. The minimum and maximum limits for this index are '0′ (no-load condition) and '1′ (system collapse condition). This LSI value for a line connected between buses i and j can be represented as (Lof et al., 1993)

$$L_{ij} = \frac{4XQ_r}{[V_i \sin(\theta - \delta_i + \delta_j)]^2} \tag{23}$$

where, X is the transmission line reactance, Q_r is the reactive power at receiving end of the transmission line, V_i is the voltage magnitude at bus-i, δ_i, δ_j are the voltage angles at the sending and receiving ends of the transmission line and θ is the impedance angle of the respective line. This index value is evaluated for each of the transmission lines. The overall system index can be considered as the maximum value among all LSI values. To install IPFC, we require two transmission line connected at common bus. By the observation of all possible locations, in this paper, by the experience, the following rules are formulated to decrease the computational effort and to increase the effectiveness of the device

1. IPFC should be connected between PQ buses only, where shunt compensators are not connected.
2. IPFC should not place in a transformer connected lines.

Table 1
Line stability index values for IEEE-30 bus system.

Location No.	IPFC			Line stability index value
	Sending end	Receiving end-1	Receiving end-2	
1	4	3	6	0.396
2	6	7	4	0.378
3	6	7	28	0.914
4	6	28	4	0.314
5	12	14	15	0.691
6	12	14	16	0.191
7	12	15	16	0.801
8	14	12	15	0.762
9	15	12	18	0.787
10	15	14	18	0.642
11	15	23	18	0.753
12	15	23	12	0.864
13	15	23	14	0.745
14	15	12	14	0.911
15	16	12	17	0.634
16	18	15	19	0.571
17	19	20	18	0.672
18	25	26	27	0.834
19	27	30	29	0.386
20	29	30	27	0.480
21	30	27	29	0.847

6. Results and analysis

To study the effect of IPFC, two different test systems namely, IEEE-30 bus and real time-23 bus test systems are considered on a computer with Intel core2Duo processor with 2GB RAM and installed with MATLAB software.

6.1. Example-1

The standard IEEE-30 bus system (Abido, 2002; Arul et al., 2013) consists six generators, forty one transmission lines, two shunt compensating devices and four tap changing transformers is considered. For this system there are twenty four control variables which include active power generations and respective voltage magnitudes at six generators, four tap settings of tap changing transformers, VAr settings of two shunt compensators and six control parameters of IPFC.

Initially, the IPFC is installed in a location obtained using the procedure described in Section 5. Using this procedure, the possible installation locations to install IPFC are twenty one. The corresponding minimized line stability index values with IPFC in each of the locations are tabulated in Table 1. From this table, it is identified that, line stability index value is less in location-6 when compared to other locations. Hence, the series converters of IPFC are placed in the lines connected between buses 12, 14 and 16 with bus-12 as common to both converters. Here, it is assumed that, the further analysis is performed by connecting IPFC in this location.

At first, the non-convex fuel cost is optimized while satisfying equality, in-equality constraints and ramp-rate limits using existing PSO and proposed MBAT algorithms. The obtained OPF results for this case are tabulated in Table 2. From this table, it is observed that, the total fuel cost value is decreased with the proposed MBAT when compared to existing PSO method. The obtained result for without ramp-rates is validated with the existing literature method (Abido, 2002). It is also observed that, with proposed MBAT algorithm, the total active power generation and there by the total power losses are increased when compared to existing PSO method. The result obtained using proposed method while satisfying system constraints and ramp-rate limits is also tabulated. In this case, it is observed that, in the presence of ramp-rate limits, the fuel cost value is increased when compared to without ramp-rate limits. At this point, the total active power generation and there by the total power losses are decreased.

Table 2
OPF results of non-convex fuel cost for IEEE-30 bus system.

S. No.	Control parameters		Existing		Proposed MBAT	
			TS (Abido, 2002)	PSO	Without Ramp-rate limits	With
1	Real power Generation (MW)	P_{G1}	200.00	193.1173	194.5512	192.3997
		P_{G2}	39.65	41.4161	46.6204	40.1383
		P_{G5}	20.42	21.0247	21.1651	19
		P_{G8}	12.47	16.0403	10	15.2051
		P_{G11}	10.00	10.3083	10	13
		P_{G13}	12.00	12	12	14
2	Generator voltages (p.u.)	V_{G1}	1.05	1.07	1.07	1.07
		V_{G2}	1.0342	1.0218	1.0508	1.0492
		V_{G5}	1.0118	1.0335	1.0322	1.0171
		V_{G8}	1.0185	1.0359	1.0509	1.0371
		V_{G11}	1.0868	0.973	1.0685	1.0058
		V_{G13}	1.0942	1.07	1.0435	1.0548
3	Transformer tap setting (p.u.)	T_{6-9}	0.9993	0.9498	1.0651	1.0199
		T_{6-10}	1.0017	1.041	1.0597	0.9864
		T_{4-12}	1.0184	1.0427	0.9749	1.082
		T_{28-27}	0.9586	0.9755	1.0273	0.998
4	Shunt compensators (MVAr)	$Q_{C,10}$	–	20.3605	21.5955	21.9342
		$Q_{C,24}$	–	14.3494	23.575	8.3619
5	Total generation (MW)		294.54	293.9067	294.3367	293.7431
6	Non-convex fuel cost ($/h)		919.72	918.253	917.9045	919.4098
7	Total power losses (MW)		11.14	10.5067	10.9367	10.3431

From this result, it is identified that, generators at buses 1, 2 are following up ramp-rates and operating toward respective maximum limits. Similarly, generators at buses 5, 8, 11 and 13 are following down ramp-rates and operating toward respective minimum limits. For example, generator at bus-3 is having P_{i0} value of 39 MW and down ramp-rate limits (DR) of 20 MW, hence this generator is operating at 19 MW (i.e. P_{i0}-DR). The same implications can be referred for other generators also. Finally, from this result, it is concluded that, in this system because of ramp-rate limits, the generators which has highest fuel cost coefficients increases their generations, hence the total fuel cost value is increased.

To validate the OPF results obtained with the proposed method are compared with some of the existing literature methods and are tabulated in Table 3. From this table, it is observed that, the proposed MBAT method yields better results when compared to other methods.

The convergence characteristics for the respective analysis are shown in Fig. 6. From this figure, it is observed that, the proposed MBAT method starts the iterative process with good initial value and reaches final best value in less number of iterations when compared to existing PSO method. System with ramp-rate limits, the initial best value and there by the number of iterations taken are increased when compared to without ramp-rate limits.

The variation of voltage magnitude at system buses with the existing and proposed methods is shown in Fig. 7. From this figure, it is observed that, voltage magnitudes get affected due to the presence of ramp-rate limits. Similarly, the variation of apparent power flow in transmission lines with existing and proposed methods is shown in Fig. 8.

Table 3
Validation of OPF results of non-convex fuel cost for IEEE-30 bus system.

S. No.	Method	Non-convex fuel cost ($/h)
1	BBO (Bhattacharya and Chattopadhyay, 2011)	919.7647
2	GSA (Serhat Duman et al., 2012)	929.72404
3	MDE (Sayah and Sehar, 2008)	930.793
4	Proposed MBAT	917.9045

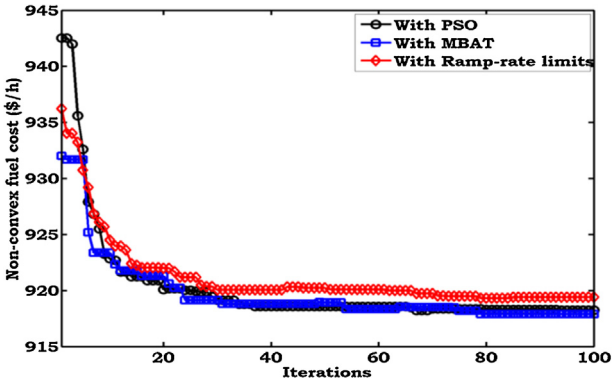

Fig. 6. Convergence characteristics of non-convex fuel cost for IEEE-30 bus system.

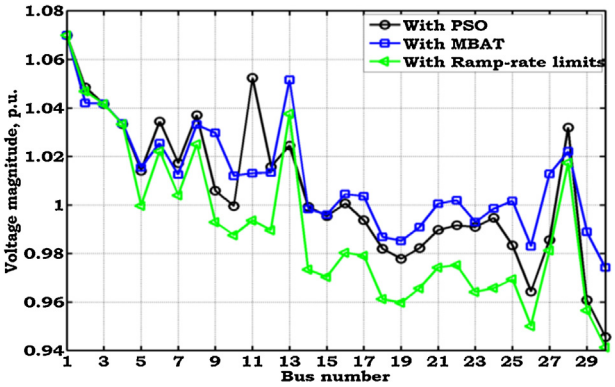

Fig. 7. Variation of bus voltage magnitudes of non-convex fuel cost for IEEE-30 bus system.

From this figure, it is observed that, because of the effectiveness of the proposed method, over loadings in some of the transmission lines is minimized.

In this analysis, to support the proposed problem formulated in Section 3, four different load levels are considered. The respective details of the considered load levels are tabulated in Table 4.

The OPF results for the considered load levels with and without IPFC are tabulated in Table 5.

At 50% load level, the total active power generation and there by the transmission losses are decreased in the presence of IPFC when compared to without device. Due to which, the total non-convex fuel cost value is decreased by 1.3461 $/h with IPFC. It is observed that, all generating units are following down ramp-rates. It is also observed

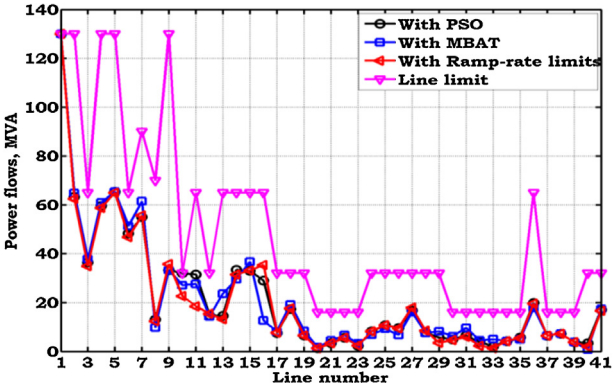

Fig. 8. Variation of power flows of non-convex fuel cost for IEEE-30 bus system.

Table 4
Demands at four Load levels for IEEE-30 bus system.

S. No.	Load level	Active power (MW)	Reactive power (MVAr)
1	50%	141.70	63.10
2	80%	226.72	100.96
3	110%	311.74	138.82
4	130%	368.42	164.06

that, except slack generator, all other units are operating at lower ramp-rate limits. For example, the initial generation value (Pio) and down ramp-rate (DR) values of generator at bus-2 are 35 MW and 10 MW, due to which, the lower ramp-rate limit for this generator is 25 MW.

At 80% load level, the total active power generation, total transmission losses and thereby the generation fuel cost values are increased when compared to values at 50% load level and these values are decreased in the presence of IPFC. Due to which, the total generation fuel cost is decreased by 1.3397 $/h. It is observed that, in this case, all generators are following down ramp-rates and operating at lower ramp-rate limits as explained in 50% load level.

At 110% load level, the total active power generation, total transmission power losses and there by the total generation fuel cost values are increased when compared to the values at 80% load level. It is observed that, total generation and total transmission losses decreased in the presence of IPFC, due to which, the total generation fuel cost value is decreased by 1.002 $/h when compared to without device. It observed that, the generators connected at buses 1, 2 and 8 buses are following up ramp-rates and whereas the generators connected at buses 5, 11 and 13 are following down ramp-rates. It is also observed that, generator at bus-13 is operating at lower ramp-rate limit i.e. (Pio-DR = 20–6 = 14 MW).

At 130% load level, the total active power generation, total transmission power losses and there by the total generation fuel cost values are increased when compared to the values at 110% load level. In this case, the total active power generation and thereby the total power losses are increased in the presence of IPFC when compared to without device, due to which the total generation fuel cost value is decreased by 3.148 $/h. It is observed that, except generator at bus-5, all other generators are following up ramp-rates. It is also observed that, generators at buses 2, 8, 11 and 13 are operating at higher ramp-rates. For example, the initial generation (Pio) at bus 2 is 35 MW and the up ramp-rate limit (UR) for this generator is 28 MW, due to which, this generator is operating at higher ramp-rate limit (Pio + UR = 35 + 28 = 63 MW).

The convergence characteristics for the considered load level are shown in Figs. 9–12. From these figures, it is observed that, in each of these cases with IPFC the iterative process starts with good initial value and reaches final best values in more number of iterations when compared to without device. This is because of the performing NR load flow in the presence of IPFC.

The consolidated variation of bus voltage magnitudes for without and with IPFC is shown in Figs. 13 and 14. From these figures, it is observed that, as the load level is increasing, bus voltage magnitudes are decreased at most of the buses.

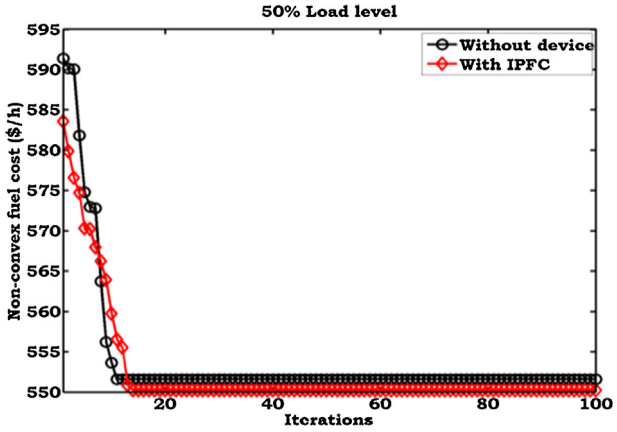

Fig. 9. Convergence characteristics of non-convex fuel cost with IPFC at 50% load level for IEEE-30 bus system.

Table 5
OPF results of non-convex fuel cost with IPFC at four load levels for IEEE-30 bus system.

S. No.	Control parameters		Load levels							
			50%		80%		110%		130%	
			Without IPFC	With IPFC	Without IPFC	With IPFC	Without IPFC	With IPFC	Without IPFC	With IPFC
1	Real power generation (MW)	P_{G1}	59.6657	59.0583	147.142	146.5927	194.7726	194.3013	192.9048	194.8191
		P_{G2}	25	25	25	25	56.0315	57.1471	63	63
		P_{G5}	19	19	19	19	21.8438	22.0945	34.182	34.5243
		P_{G8}	15	15	15	15	23.7939	21.7677	30	30
		P_{G11}	13	13	13	13	13.0686	13.7617	28	28
		P_{G13}	14	14	14	14	14	14	35	35
2	Generator voltages (p.u.)	V_{G1}	1.0435	1.0253	1.0548	1.0989	1.07	1.1	1.0533	1.0977
		V_{G2}	1.0336	0.9893	0.9931	1.0749	1.0417	0.9933	0.9699	0.95
		V_{G5}	1.07	1.0446	1.0193	0.9888	1.0001	1.0781	1.0074	1.0285
		V_{G8}	1.0101	0.9694	1.0097	1.0532	1.031	1.0701	1.0414	1.031
		V_{G11}	1.0406	1.0391	0.9972	1.0146	1.0557	1.0477	1.0695	1.0327
		V_{G13}	0.9775	0.954	0.9627	1.0183	1.0178	1.0857	1.062	1.0715
3	Transformer tap setting (p.u.)	T_{6-9}	0.9	0.9	0.9853	0.961	1.0539	0.9468	1.0119	1.0054
		T_{6-10}	0.9	1.0558	0.9384	1.0493	1.0083	1.0305	0.9837	0.9454
		T_{4-12}	1.0385	1.0218	0.9045	0.9	1.0363	1.0117	1.0823	0.9922
		T_{28-27}	0.9353	0.9005	0.927	0.9636	1.0349	1.0068	0.9534	0.9882
4	Shunt compensators (MVAr)	$Q_{C,10}$	22.5458	13.1087	21.9037	28.0188	7.2297	16.2166	19.4861	16.9294
		$Q_{C,24}$	14.7159	8.5576	19.8268	11.3418	18.6042	21.9908	15.3908	17.6271
5	IPFC control parameters	$r_{ij}, p.u.$	–	0.0472	–	0.0184	–	0.0012	–	0.0281
		$r_{ik}, p.u.$	–	0.0185	–	0.0267	–	0.0277	–	0.0355
		r_{ij}, deg	–	270.281	–	15.8692	–	36	–	304.0648
		r_{ik}, deg	–	0.9698	–	147.0205	–	77.927	–	65.7529
		$X_{se,ij}, p.u.$	–	0.0876	–	0.0414	–	0.0437	–	0.0812
		$X_{se,ik}, p.u.$	–	0.0384	–	0.1	–	0.0681	–	0.0769
6	Total generation (MW)		145.6657	145.0583	233.142	232.5927	323.5104	323.0723	383.0868	385.3434
7	Non-convex fuel cost ($/h)		551.5657	550.2196	755.2588	753.9191	1021.112	1020.11	1274.494	1271.346
8	Total power loss (MW)		3.9657	3.3583	6.422	5.8727	11.7704	11.3323	14.6668	16.9234

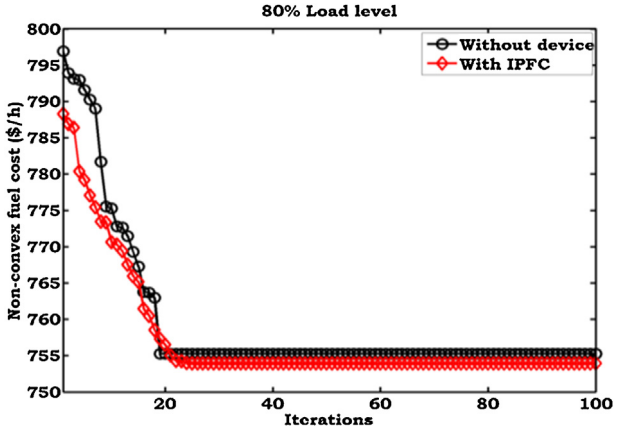

Fig. 10. Convergence characteristics of non-convex fuel cost with IPFC at 80% load level for IEEE-30 bus system.

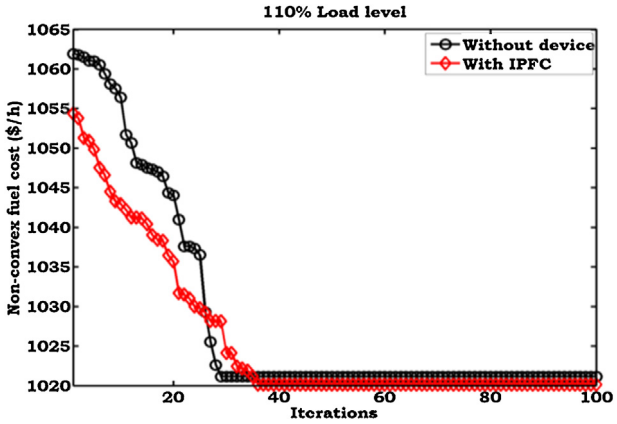

Fig. 11. Convergence characteristics of non-convex fuel cost with IPFC at 110% load level for IEEE-30 bus system.

6.2. *Example-2*

The real-time 23 bus system consists ten generators, twenty eight transmission lines, six shunt compensating devices and five tap changing transformers is considered. For this system there are thirty seven control variables which

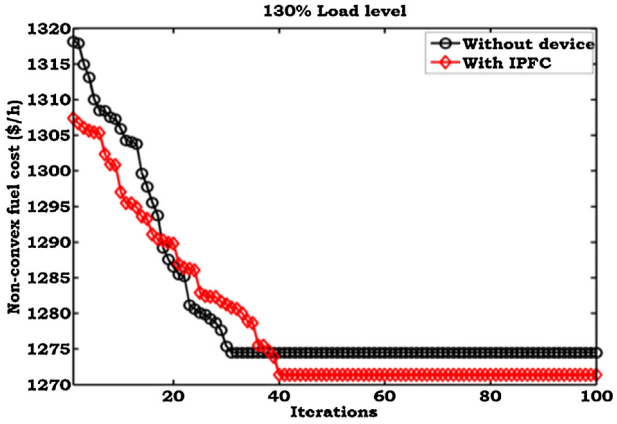

Fig. 12. Convergence characteristics of non-convex fuel cost with IPFC at 130% load level for IEEE-30 bus system.

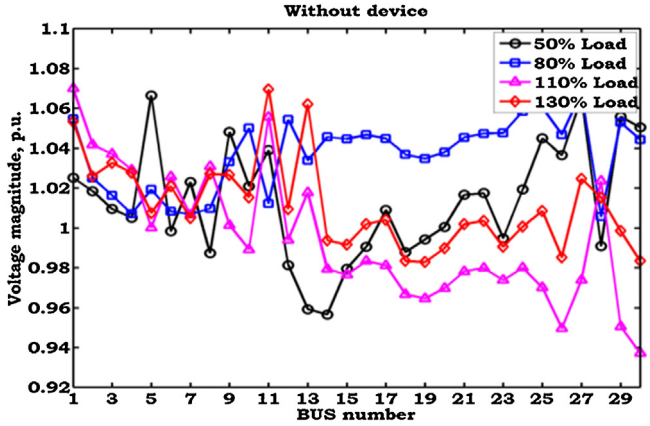

Fig. 13. Variation of bus voltage magnitudes of non-convex fuel cost without IPFC at four load levels for IEEE-30 bus system.

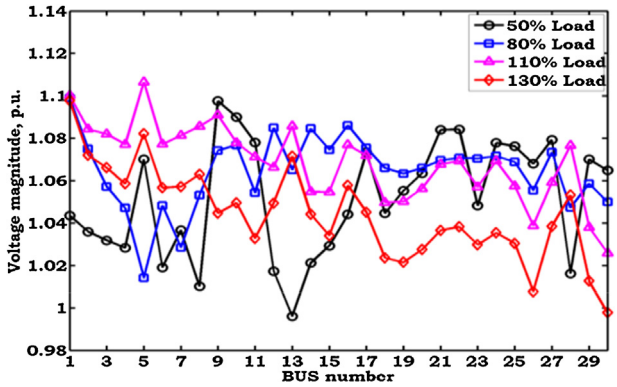

Fig. 14. Variation of bus voltage magnitudes of non-convex fuel cost with IPFC at four load levels for IEEE-30 bus system.

include active power generations and respective voltage magnitudes at ten generators, five tap settings of tap changing transformers, VAr settings of six shunt compensators and six control parameters of IPFC.

Initially, the IPFC is installed in a location obtained using the procedure described in Section 5. Using this procedure, the possible installation locations to install IPFC are two. The corresponding minimized line stability index values with IPFC in each of the locations are tabulated in Table 6. From this table, it is identified that, line stability index value is less in location-1 when compared to other location. Hence, the series converters of IPFC are placed in the lines connected between buses 12, 11 and 23 with bus-12 as common to both converters. Here, it is assumed that, the further analysis is performed by connecting IPFC in this location.

At first, the non-convex fuel cost is optimized while satisfying equality, in-equality constraints and ramp-rate limits using existing PSO and proposed MBAT algorithms. The obtained OPF results for this case are tabulated in Table 7. From this table, it is observed that, the total fuel cost value is decreased with the proposed MBAT when compared to existing PSO method. It is also observed that, with proposed MBAT method, the total active power generation and there by the total power losses are decreased when compared to existing PSO method. The result obtained using proposed

Table 6
Line stability index values for real-time 23 bus system.

Location No.	IPFC			Line stability index value
	Sending end	Receiving end-1	Receiving end-2	
1	12	11	23	10.7841
2	10	11	18	15.2080

Table 7
OPF results of non-convex fuel cost for real-time 23bus system.

S. No.	Control parameters		Existing PSO	Proposed MBAT	
				Without ramp-rate limits	With ramp-rate limits
1	Real power generation (MW)	P_{G1}	425.6537	462.4859	497.6139
		P_{G3}	421.6457	344.8792	329.0127
		P_{G5}	459.9548	389.5022	456.071
		P_{G6}	344.5171	336.0179	244.8964
		P_{G9}	425.6857	357.3421	336.0983
		P_{G13}	482.114	484.529	476.6406
		P_{G14}	714.2417	782.6488	969.7755
		P_{G17}	496.6353	543.2837	496.6152
		P_{G21}	182.5077	196.3057	148.7781
		P_{G22}	663.9784	700.8947	668.2578
2	Generator voltages (p.u.)	V_{G1}	1.0118	1.0243	0.9786
		V_{G3}	1.0175	1.0282	0.9755
		V_{G5}	0.9481	0.9858	0.9019
		V_{G6}	1.047	1.0486	1.012
		V_{G9}	1.0763	1.0057	1.0464
		V_{G13}	1.0764	0.9816	0.9408
		V_{G14}	1.0462	1.0658	1.0198
		V_{G17}	0.9896	0.9976	0.954
		V_{G21}	1.0329	1.0961	0.9256
		V_{G22}	1.0082	0.9874	0.9285
3	Transformer tap setting (p.u.)	T_{3-10}	1.0306	1.0106	1.0209
		T_{8-12}	1.0447	1.0026	1.0433
		T_{5-11}	0.9501	1.0305	0.995
		T_{14-18}	0.9593	0.9572	0.9588
		T_{22-23}	1.0624	1.008	1.0089
4	Shunt compensators (MVAr)	$Q_{C,2}$	14.167	21.2262	19.6607
		$Q_{C,5}$	6.1316	19.4842	16.8247
		$Q_{C,13}$	25.1017	14.456	24.4478
		$Q_{C,15}$	18.0356	26.1038	8.7449
		$Q_{C,16}$	22.6859	16.7531	22.5283
		$Q_{C,21}$	20.6316	17.7542	18.7567
5	Total generation (MW)		2559.571	2374.756	2340.333
6	Non-convex fuel cost (Rs/h)		50 686.35	50 619.04	51 463.32
7	Total power loss (MW)		166.934	147.8891	173.7595

method while satisfying system constraints and ramp-rate limits is also tabulated. In this case, it is observed that, in the presence of ramp-rate limits, the fuel cost value is increased when compared to without ramp-rate limits. At this point, the total active power generation is decreased and the total power losses are increased.

From this result, it is identified that, all generators except generator at bus-9 are following up ramp-rates and operating toward respective maximum limits. Similarly, generator at bus 9 is following down ramp-rates and operating toward respective minimum limits. Finally, from this result, it is concluded that, in this system because of ramp-rate

Table 8
Demands at four Load levels for real-time 23 bus system.

S. No.	Load level	Active power (MW)	Reactive power (MVAr)
1	50%	2225	557.5
2	80%	3560	892
3	110%	4895	1226.5
4	120%	5340	1338

Table 9
OPF results of non-convex fuel cost with IPFC at four load levels for real-time 23 bus system.

S. No.	Control parameters		Load level							
			50%		80%		110%		120%	
			Without IPFC	With IPFC	Without IPFC	With IPFC	Without IPFC	With IPFC	Without IPFC	With IPFC
1	Real power generation (MW)	P_{G1}	368.1704	378.0946	374.0744	378.1659	475.3085	481.4904	589.105	591.9442
		P_{G3}	156.984	160.2192	282.2179	292.3681	427.3115	427.9632	509.95	499.6015
		P_{G5}	200	200	321.8193	323.6689	508.337	509.8097	540.8086	551.6368
		P_{G6}	100	104.0263	250.7256	254.5564	273.3715	277.2532	342.4042	342.9499
		P_{G9}	208.8083	200	333.784	333.9927	529.0867	515.634	523.7869	503.2219
		P_{G13}	231.4632	231.5017	362.0602	367.9768	531.9896	530.2947	600	600
		P_{G14}	300	312.8702	542.5816	547.7669	957.9116	948.9394	958.2237	961.355
		P_{G17}	309.4243	300	544.6424	524.5883	479.8432	487.2247	597.3739	600
		P_{G21}	86.3069	87.2656	113.6359	123.6324	155.9347	165.6101	152.0332	166.3448
		P_{G22}	311.2331	300	520.4544	506.3663	725.0124	725.9059	800	800
2	Generator voltages (p.u.)	V_{G1}	1.0101	1.004	1.0194	1.0293	0.9399	0.9634	1.0144	0.9498
		V_{G3}	1.0135	0.9552	1.0197	1.0353	0.9524	0.9853	1.0466	0.9965
		V_{G5}	1.069	0.9988	1.0024	0.9771	1.0092	0.9794	0.9865	0.9873
		V_{G6}	0.9816	1.0412	1.0406	1.0371	0.9769	0.9835	1.0241	0.9561
		V_{G9}	1.0183	1.0445	1.0198	1.0012	1.0086	1.01	1.0366	0.9796
		V_{G13}	0.9997	0.9592	1.0353	0.967	0.9677	1.0554	1.0113	1.0391
		V_{G14}	0.9563	1.0662	1.0412	1.0144	1.0308	0.9486	1.0548	1.001
		V_{G17}	1.0122	1.0549	0.982	0.9377	1.07	0.9889	1.0576	0.9505
		V_{G21}	1.0029	1.069	0.9568	0.9254	1.0202	1.015	0.925	1.0206
		V_{G22}	0.9991	1.0865	1.0038	0.9668	1.0437	1.0595	0.993	1.0236
3	Transformer tap setting (p.u.)	T_{3-10}	0.9762	0.9101	1.0435	1.0723	0.9858	0.9782	1.031	1.0154
		T_{8-12}	0.933	0.9611	1.0022	0.9898	0.959	1.0313	0.9827	0.9947
		T_{5-11}	1.0182	0.9591	0.9622	0.9779	0.9946	0.979	1.0143	0.9978
		T_{14-18}	0.9484	0.9243	1.025	1.0276	0.9	1.0262	0.9407	1.0731
		T_{22-23}	0.9603	0.9773	0.98	1.0161	1.044	1.0313	0.9788	1.0606
4	Shunt compensators (MVAr)	$Q_{C,2}$	9.3897	17.5461	12.8461	15.8638	21.6795	13.6281	23.6601	19.8329
		$Q_{C,5}$	19.3103	28.8451	28.5095	20.6846	11.8467	13.4669	27.2104	24.6521
		$Q_{C,13}$	7.5659	19.6366	17.1538	19.3458	21.48	23.943	12.9483	26.7537
		$Q_{C,15}$	5.1957	7.5003	15.0933	14.3962	14.8054	6.4525	20.7714	7.8134
		$Q_{C,16}$	20.3317	26.058	18.5703	23.808	9.9516	13.3852	21.8907	16.9124
		$Q_{C,21}$	10.335	23.288	21.4132	19.6787	8.5285	25.9518	22.93	22.4133
5	IPFC control parameters	$r_{ij}, p.u.$	–	0.011	–	0.0457	–	0.0365	–	0.0433
		$r_{ik}, p.u.$	–	0.0713	–	0.0831	–	0.0502	–	0.0436
		r_{ij}, deg	–	308.5847	–	291.0041	–	281.3541	–	168.7081
		r_{ik}, deg	–	147.2194	–	247.5832	–	268.1024	–	266.6673
		$X_{se,ij}, p.u.$	–	0.0261	–	0.0734	–	0.0689	–	0.0651
		$X_{se,ik}, p.u.$	–	0.0205	–	0.0542	–	0.0348	–	0.0741
6	Total generation (MW)		2272.39	2273.978	3645.996	3653.083	5064.107	5070.125	5613.686	5617.054
7	Non-convex fuel cost (Rs/h)		21 785.98	21 763.23	38 280.07	38 168.5	57 590.15	57 438.18	65 754.76	65 743.83
8	Total power loss (MW)		47.3902	48.9776	85.9957	93.0827	169.1067	175.1253	273.6855	277.0541

limits, the generators which has highest fuel cost coefficients increases their generations, hence the total fuel cost value is increased.

To support the proposed problem formulated in Section 4, four different load levels are considered. The respective details of the considered load levels are tabulated in Table 8.

The OPF results for the considered load levels with and without IPFC are tabulated in Table 9. At 50% load level, the total active power generation and there by the transmission losses are increased in the presence of IPFC when compared to without device. Due to which, the total non-convex fuel cost value is decreased by 230.4 Rs/h with IPFC. It is observed that, all generating units are following down ramp-rates. It is also observed that, the generators connected at buses 5, 6, 9 and 14 are operating at lower ramp-rate limits. For example, the initial generation value (Pio) and down ramp-rate (DR) values of generator at bus-5 are 400 MW and 200 MW, due to which, the lower ramp-rate limit for this generator is 200 MW.

At 80% load level, the total active power generation, total transmission losses and thereby the generation fuel cost values are increased when compared to values at 50% load level and these values are increased in the presence of IPFC. Due to which, the total generation fuel cost is decreased by 111.57 Rs/h. It is also observed that, in this case, the generators at buses 1, 3 and 9 are following down ramp-rates and the remaining generators are following up ramp-rates.

At 110% load level, the total active power generation, total transmission power losses and there by the total generation fuel cost values are increased when compared to the values at 80% load level. It is observed that, total generation and total transmission losses increased in the presence of IPFC, due to which, the total generation fuel cost value is decreased by 151.97 Rs/h when compared to without device. It observed that, except slack generator all other generators are following up ramp-rates and whereas slack generator is following down ramp-rate limit.

At 120% load level, the total active power generation, total transmission power losses and there by the total generation fuel cost values are increased when compared to the values at 110% load level. In this case, the total active power generation and thereby the total power losses are increased in the presence of IPFC when compared to without device, due to which the total generation fuel cost value is decreased by 10.93 Rs/h. It is observed that, all generators are following up ramp-rates. It is also observed that, generators at buses 13, 17 and 22 are operating at generation maximum limits even though higher ramp-rate limit is greater than maximum limit. For example, the initial generation (Pio) at bus 22 is 500 MW and the up ramp-rate limit (UR) for this generator is 400 MW, due to which, this generator is operating at maximum limit (800 MW) i.e. Pio + UR = 500 + 400 = 900 MW.

The similar observations can be interpreted for convergence characteristics, variation of active power generations, voltage magnitudes and power flows as explained for the previous example. Due to pagination problem, the similar type of graphical results cannot able to provide for this example.

7. Conclusion

In this paper, OPF problem has been solved under dynamic load conditions with non-convex fuel cost as an objective while satisfying system equality, inequality and ramp-rate limits without and with IPFC. Four different load levels have been considered with increase of active and reactive loads by same factor, to resemble minimum, base, average and peak load conditions over a specified period on power system. The effectiveness of these dynamic loads on system parameters such as active power generations and voltage magnitudes has been analyzed. The effect of ramp-rate limits on generators has been also exemplified with necessary explanations. From the analysis, it has been observed that, as the load on a system is increasing the active power generation by the generators is also increasing. Due to which, the total active power generation and there by the losses are also increased as load level has been increased. Finally, the bus voltage magnitudes are enhanced in the presence of IPFC when compared to without device. The proposed methodology has been tested on standard IEEE-30 bus and real time 23 bus test systems with supporting numerical and graphical results. In future, there is a scope to extend the same work by considering different load levels with different incremental factors to increase active and reactive loads to resemble realistic loads on a system.

Appendix.

The modifications in power mismatch and Jacobian elements at IPFC connected bused can be derived as follows:

A.1. Modifications in power mismatch equations

The power mismatch equations at the IPFC connected buses can be modified by adding the IPFC injected powers to the power mismatch equations without device. These power mismatch equations can be expressed as

$$\Delta P_m^{IPFC} = \Delta P_m^0 + P_m^{IPFC}; \quad \forall m = i, j, k$$

$$\Delta Q_m^{IPFC} = \Delta Q_m^0 + Q_m^{IPFC}; \quad \forall m = i, j, k$$

A.2 Modifications in Jacobian elements

The diagonal and off-diagonal elements of 'H^{IPFC}' are

$$H_{ii}^{IPFC} = \frac{\partial P_i^{IPFC}}{\partial \delta_i} = 0$$

$$H_{mm}^{IPFC} = \frac{\partial P_m^{IPFC}}{\partial \delta_m} = -Q_m^{IPFC}; \quad m = j, k$$

$$H_{mi}^{IPFC} = \frac{\partial P_m^{IPFC}}{\partial \delta_i} = Q_m^{IPFC}; \quad m = j, k$$

Similarly, the diagonal and off-diagonal elements of 'N^{IPFC}' are

$$N_{mi}^{IPFC} = |V_i| \frac{\partial P_m^{IPFC}}{\partial V_i} = 0$$

$$N_{mm}^{IPFC} = |V_m| \frac{\partial P_m^{IPFC}}{\partial V_m} = P_m^{IPFC}; \quad m = j, k$$

$$N_{mm}^{IPFC} = |V_m| \frac{\partial P_m^{IPFC}}{\partial V_m} = 0; \quad m = j, k$$

$$N_{mi}^{IPFC} = |V_i| \frac{\partial P_m^{IPFC}}{\partial V_i} = P_m^{IPFC}; \quad m = j, k$$

The diagonal and off-diagonal elements of 'J^{IPFC}' are

$$J_{ii}^{IPFC} = \frac{\partial Q_i^{IPFC}}{\partial \delta_i} = 0$$

$$J_{mm}^{IPFC} = \frac{\partial Q_m^{IPFC}}{\partial \delta_m} = P_m^{IPFC}; \quad m = j, k$$

$$J_{im}^{IPFC} = \frac{\partial Q_i^{IPFC}}{\partial \delta_m} = 0; \quad m = j, k$$

$$J_{mi}^{IPFC} = \frac{\partial Q_m^{IPFC}}{\partial \delta_i} = -P_m^{IPFC}; \quad m = j, k$$

Similarly, the diagonal and off-diagonal elements of 'L^{IPFC}' are

$$L_{ii}^{IPFC} = |V_i| \frac{\partial Q_i^{IPFC}}{\partial V_i} = 2Q_i^{IPFC}$$

$$L_{mm}^{IPFC} = |V_m| \frac{\partial Q_m^{IPFC}}{\partial V_m} = Q_m^{IPFC}; \quad m = j, k$$

$$L_{im}^{IPFC} = |V_m| \frac{\partial Q_i^{IPFC}}{\partial V_m} = 0; \quad m = j, k$$

$$L_{mi}^{IPFC} = |V_i| \frac{\partial Q_m^{IPFC}}{\partial V_i} = Q_m^{IPFC}; \quad m = j, k$$

References

Abido, M.A., 2002. Optimal power flow using Tabu search algorithm. Electr. Power Comp. Syst. 30, 469–483.

Acha, E., Fuerte-Esquivel, C.R., Ambriz-perez, H., Angeles-Camacho, C., 2004. FACTS Modeling and Simulation in Power Networks. John Wiley and Sons, Chichester, England.

Arul, R., Ravi, G., Velusami, S., 2013. Non-convex economic dispatch with heuristic load patterns, valve point effect, prohibited operating zones, ramp-rate limits and spinning reserve constraints using harmonic search algorithm. Electr. Eng. 95, 53–61.

Attaviriyanupap, D., Kita, H., Tanaka, E., Hasegawa, J., 2002. A hybrid EP and SQP for dynamic economic dispatch with non smooth incremental fuel cost function. IEEE Trans. Power Syst. 17 (2), 411–416.

Baskar, G., Mohan, M.R., 2008. Security constrained economic load dispatch using improved particle swarm optimization suitable for utility system. Int. J. Electr. Power Energy Syst. 30 (10), 609–613.

Belwin Edward, J., Rajasekar, N., Sathiyasekar, K., Senthilnathan, N., Sarjila, R., 2013. An enhanced bacterial foraging algorithm approach for optimal power flow problem including FACTS devices considering system loadability. ISA Trans. 52, 622–628.

Bhattacharya, A., Chattopadhyay, P.K., 2011. Application of biogeography-based optimization to solve different optimal power flow problems. IET Gener. Transm. Distrib. 5 (1), 70–80.

Bhowmick, S., Das, B., Kumar, N., 2008. An indirect UPFC model to enhance reusability of Newton power flow codes. IEEE Trans. Power Deliv. 23 (4), 2079–2088.

Chung, T.S., Li, Y., 2001. A hybrid GA approach for OPF with consideration of FACTS devices. IEEE Power Eng. Rev. 21 (2), 47–50.

Deng, w., Lie, T.T., 1995. Optimal compensation of variable series capacitors for improved economic dispatch in power systems. In: Proc. of International Conference on Energy Management and Power Delivery, vol. 2, pp. 732–737.

Douglas, J., Gotham, G., Heydit, T., 1998. Power flow control and power flow studies for systems with FACTS devices. IEEE Trans. Power Syst. 13 (1), 60–65.

Fuerte-Esquivel, C.R., Acha, E., 1996. Newton–Raphson algorithm for the reliable solution of large power networks with embedded FACTS devices. IEEE Proc. Gener. Trans. Distrib. 143 (5), 447–454.

Gotham, D.J., Heydt, G.T., 1998. Power flow control and power flow studies for systems with FACTS Devices. IEEE Trans. Power Syst. 13 (1).

Hao, Z.F., Guo, G.H., Huang, H., 2007. A particle swarm optimization algorithm with differential evolution. IEEE Int. Conf. Syst. Man Cybern. 2, 1031–1035.

Hindi, K.S., Ab Ghani, M.R., 1991. Dynamic economic dispatch for large scale power systems: a Lagrangian relaxation approach. Int. J. Electr. Power Energy 13 (1), 51–56.

Hingorani, N.G., 1988. Power electronics utilities: role of power electronics in future power systems. In: Proc. of the IEEE, vol. 76, no. 4, pp. 481–482.

Hingorani, N.G., Gyugyi, L., 1999. Understanding FACTS: Concepts and Technology of Flexible AC Transmission Systems. IEEE Press, New York.

Zhang, Jun, Yokoyama, Akihiko, 2006a. Optimal power flow control for congestion management by interline power flow controller. In: IEEE Int. Conf. on Power System Technology, Chongqing, China, pp. 1–6.

Jun, Zhang, Yokoyama, A., 2006b. A comparison between the UPFC and the IPFC in optimal power flow control and power flow regulation. In: Proc. of IEEE Int. Conf, pp. 339–345.

Kirschner, L., Retzmann, D., Thumm, G.,2005. Benefits of FACTS for power system enhancement. In: Distribution Conference and Exhibition. IEEE, pp. 1–7.

Kumari, M.S., Priyanka, G., Sydulu, M., 2007. Comparison of Genetic algorithms and particle swarm optimization for optimal power flow including FACTS devices. In: IEEE Power Tech. Conference, Lausanne, pp. 1105–1110.

Lof, P.A., Andersson, G., Hill, D.J., 1993. Voltage stability indexes for stressed power system. IEEE Trans. Power Syst. 8 (1), 326–334.

Ongsakul, W., Bhasaputra, P., 2002. Optimal power flow with FACTS devices by hybrid TS/SA approach. Electr. Power Energy Syst. 24, 851–857.

Padhy N.P., Abdel Moamen, M.A., 2005. Power flow control and solutions with multiple and multi-type FACTS devices. Electr. Power Syst. Res. 74 (3), 341–351.

Panigraphi, C.K., Chattopadhyay, P.K., Chakrabarti, R.N., Basu, M., 2006. Simulated annealing technique for dynamic economic dispatch. Electr. Power Comp. Syst. 34 (5), 577–586.

Perez, M.A., Messina, A.R., Fuerte-Esquivel, C.R.,2000. Application of FACTS devices to improve steady state voltage stability. In: Power Engineering Society Summer Meeting, vol. 2. IEEE, pp. 1115–1120.

Pilotto, L.A.S., Ping, W.W., Carvalho, A.R., Wey, A., et al., 1997. Determination of needed FACTS controllers that increase asset utilization of power systems. IEEE Trans. Power Deliv. 12 (1), 364–371.

Sauer, P.W., Lesientre, B.C., Pai, M.A., 1993. Maximum loadability and voltage stability in power system. Int. J. Electr. Power Energy Syst. 15 (3), 145–154.

Sayah, S., Sehar, K., 2008. Modified differential evolution algorithm for optimal power flow with non-smooth cost functions. Energy Convers. Manag. 49, 3036–3042.

Duman, S., Guvenc, U., Sonmez, Y., Yorukeren, N., 2012. Optimal power flow using gravitational search algorithm. Energy Convers. Manag. 59, 86–95.

Shanti Swarup, K., Natrajan, A., 1994. Constrained optimization using economic dispatch. Proc. Inst. Elect. Eng. Gener. Transm. Distrib. 141 (5), 507–513.

Singh, S.N., David, A.K., 2001. A new approach for placement of FACTS devices in open power markets. IEEE Power Eng. Rev. 21 (9), 58–60.

Taranto, G.N., Pinto, L.M.V.G., Pereira, M.V.F., 1992. Representation of FACTS devices in a power system economic dispatch. IEEE Trans. Power Syst. 7 (2), 572–576.

Teerathana, S., Yokoyama, A., Nakachi, Y., Yasumatsu, M., 2005. An optimal power flow control method of power system by interline power flow controller. In: Proc. of 7th Int. Power Eng. Conf., Singapore, pp. 1–6.

Titus, S., Ebenezer Jeyakumar, A., 2008. A hybrid EP-PSO-SQP algorithm for dynamic dispatch considering prohibited operating zones. Electr. Power Comp. Syst. 36 (5), 449–467.

Vinkovic, A., Mihalic, R., 2008. A current-based model of SSSC for Newton Raphson power flow. Electr. Power Syst. Res. 78, 1806–1813.

Vinkovic, A., Mihalic, R., 2009. A current-based model of an IPFC for Newton Raphson power flow. Electr. Power Syst. Res. 79, 1247–1254.

Xia Jiang, X., Fang, J.H., Chow, A.A., Edris, E. Uzunovic, et al., 2008. A novel approach for modeling voltage sourced converter based FACTS controllers. IEEE Trans. Power Deliv. 23 (4), 2591–2598.

Xiao, Y., Song, Y.H., Sun, Y.Z., 2002. Power Flow Control Approach to Power Systems, vol. 17, no. 4, pp. 943–950.

Xingbin, Y.U., Jakovljevic, S., Ristanovic, D., Hung, Gang,2003. Total transfer capability considering FACTS and security constraints. In: Transmission and Distribution Conference and Exposition, vol. 1. IEEE, pp. 73–78.

Xinghao, Fang, Chow, J.H., Jiang, Xia, Fardanesh, B., Uzunovic, E., Edris, A.A., 2009. Sensitivity methods in the dispatch and sitting of FACTS controllers. IEEE Trans. Power Syst. 24 (2), 713–720.

Yang, Xin-She, He, Xingshi, 2013. Bat algorithm: literature review and applications. Int. J. Bioinspir. Comput. 3 (3), 141–149.

Yan, P., Sekar, A., 2005. Steady state analysis of power system having multiple FACTS devices using line-flow based equations. IEEE Proc. Transm. Distrib. 152 (1), 31–39.

Yan, O., Singh, C.,2001. Improvement of total transfer capability using TCSC and SVC. In: Power Engineering Society Summer Meeting, vol. 2. IEEE, pp. 944–948.

Yankui, Zhang, Zhang, Yan, Chen, Chen, 2006. A novel power injection model of IPFC for power flow analysis inclusive of practical constraints. IEEE Trans. Power Syst. 21 (4), 1550–1556.